

Quark model description of $\psi(4260)$

R. Bruschini* and P. González†

Departamento de Física Teórica-IFIC
 Universidad de Valencia-CSIC
 E-46100 Burjassot(Valencia), Spain

Abstract

From lattice indications we follow a Born-Oppenheimer approximation to build a quark-antiquark static potential for $J^{PC} = 1^{--}$ charmonium states below their first S- wave meson-meson threshold. We show that a good description of the mass and decay properties of the experimentally well established $\psi(4260)$ resonance is feasible.

Keywords: quark; meson; potential.

1 Introduction

The explanation of experimentally discovered charmonium states, that do not fit well in conventional quark model descriptions of heavy quarkonia as for instance the ones provided by the Cornell [1, 2] or the Godfrey-Isgur [3] models, is nowadays a theoretical challenge.

Regarding unconventional isospin 0 states ($\chi_{c1}(3872)$, $\psi(4260)$...), see [4], the presence of close open flavor (charm) meson-meson thresholds may be playing an important role. As a matter of fact explanations involving the presence of meson-meson components in the form of either molecules, or tetraquarks implicitly involving several molecular configurations, or complementary configurations to the heavy quark-antiquark ones have been developed (for recent bibliographic reviews see [5], [6], [7], [8] and references therein; for a more general heavy quarkonia review see [9]).

*roberto.bruschini@ific.uv.es

†pedro.gonzalez@uv.es

One possible alternative explanation may come from the consideration of a “beyond the conventional” quark model description, where the meson-meson degrees of freedom as well as the gluon ones are integrated out through an effective heavy quark-antiquark potential. A specific form for this potential can be proposed from lattice calculations [10] for the energy of two static color sources (quark Q and antiquark \bar{Q}) when mixing of the $Q\bar{Q}$ configuration with an open flavor meson-meson one is taken into account. By using a Born-Oppenheimer approximation the resulting $Q\bar{Q}$ static potential below the meson-meson threshold exhibits screening starting at a certain energy below the threshold and saturating (becoming flat) at the threshold mass.

The screening energy interval is shorter for $Q\bar{Q}$ configurations ($Q = b$ or c) involving only mesons with very small widths (B, B^* or D, D^*). From lattice results the starting screening energy in this case may be estimated to be about 30 MeV below the threshold mass. In a first approach one may tentatively take the simplifying assumption that screening takes place just at the threshold mass (zero screening energy interval approach). This idea has been implemented and extended through the so called Generalized Screened Potential Model for the description of $0^+(J^{++})$ charmonium ($J = 0, 1, 2$) [11, 12] as well as bottomonium states [13].

When applied to $0^-(1^{--})$ charmonium this approach fails even in the low energy spectral region below the first S - wave meson-meson threshold that we shall call henceforth $D\bar{D}_1$ (involving $D\bar{D}_1(2420)$ and $D\bar{D}_1(2430)$) since the unconventional $\psi(4260)$ can not be sensibly assigned to any state from the potential. This failure may have to do with the need of implementing a non zero screening energy interval in this case due to the significant threshold width.

In this article we try to go a step further in the construction of the potential for $0^-(1^{--})$ charmonium by implementing a non zero screening energy interval. We shall show that a reasonable description of $0^-(1^{--})$ states lying below the $D\bar{D}_1$ threshold including $\psi(4260)$ may be attained. The contents of the article are organized as follows. In Section 2 a brief review of the (zero screening energy interval approach) potential for $0^+(1^{++})$ states below their first S - wave meson-meson threshold is presented. In Section 3 we implement the potential for $0^-(1^{--})$ states. From it we calculate the spectrum below their first S - wave meson-meson threshold. In Section 4 we concentrate on the study of $\psi(4260)$, the only well established unconventional state in this spectral region. We calculate its decay properties and compare them to existing data. Finally in Section 5 our main results and conclusions are summarized.

2 $c\bar{c}$ Potential for $0^+(1^{++})$ states

In order to construct a $Q\bar{Q}$ static potential implicitly incorporating the effect of meson-meson components we shall start from (unquenched) lattice results [10] for the energy of two static color sources (Q and \bar{Q}) when mixing of the $Q\bar{Q}$ configuration with an open flavor meson-meson one is taken into consideration. As a consequence of the presence of this meson-meson configuration the $Q\bar{Q}$ static energy changes its radial dependence on the $Q - \bar{Q}$ distance. Following a Born-Oppenheimer interpretation we shall identify the $Q\bar{Q}$ static energy with the $Q\bar{Q}$ static potential (for a review of Born-Oppenheimer potentials see [14]).

For the sake of clarity let us go step by step. First let us only consider a $Q\bar{Q}$ configuration. The dependence of the $Q\bar{Q}$ static energy on the $Q - \bar{Q}$ distance has been derived in (quenched) lattice QCD [15]. By identifying this energy dependence with the (quenched) $Q\bar{Q}$ static potential one gets a Cornell like form

$$V_C(r) = \sigma r - \frac{\zeta}{r} \quad (1)$$

where r is the $Q - \bar{Q}$ distance and the parameters σ and ζ stand for the string tension and the chromoelectric coulomb strength respectively. This potential is drawn in Fig. 1 where the values of the parameters

$$\begin{aligned} \sigma &= 850 \text{ MeV/fm} \\ \zeta &= 100 \text{ MeV.fm} \\ m_c &= 1348.6 \text{ MeV} \\ m_b &= 4793 \text{ MeV} \end{aligned} \quad (2)$$

have been chosen to get a reasonable fit of the low lying $0^+(J^{++})$ charmonium and bottomonium spectra [11, 13].

Let us now consider a $Q\bar{Q}$ configuration with quantum numbers $I^G(J^{PC})$, for example $0^+(1^{++}) c\bar{c}$, plus a meson-meson configuration. It is important to realize that the first open flavor meson-meson configuration with these quantum numbers that may contribute to the static potential is $D^0\bar{D}^{*0}$ (from now on it is always understood that the sum of the charge conjugate meson-meson configuration is implicit). This is so, despite the fact that $D^0\bar{D}^0$ has a lower energy threshold, because the two mesons have to be in an S -wave channel for the c quark in one meson and the \bar{c} antiquark in the other meson to remain static as required (this is only strictly true in the infinite c mass limit, $m_c \rightarrow \infty$, but it can be taken as a good approximation). (Actually, $D^0\bar{D}^0$ is the first threshold contributing to the $0^+(0^{++})$ static potential.)

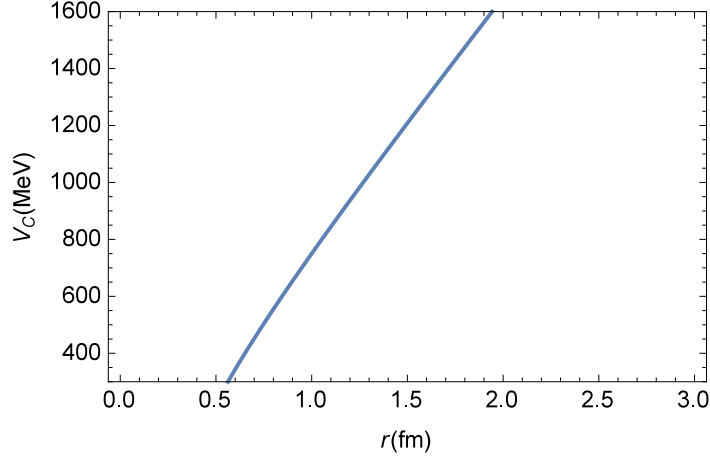


Figure 1: Representation of the static potential $V_C(r)$ with $\sigma = 850$ MeV/fm and $\zeta = 100$ MeV.fm.

From lattice results obtained when a $Q\bar{Q}$ and a meson-meson configurations are considered [10] we expect $c\bar{c}$ and $D\bar{D}^*$ mixing (for simplicity we assume the same mass for the different isospin components and call the threshold $D\bar{D}^*$). This makes the formal dependence of the $c\bar{c}$ static energy on the $c - \bar{c}$ distance to be different close below and above the threshold mass. In particular, this dependence starts to differ from the Cornell like form when approaching the meson-meson threshold from below becoming flat at the threshold mass. If this change takes place in a small energy region then the identification of this energy dependence with a (unquenched) $0^+(1^{++})$ $c\bar{c}$ static potential gives rise to the approximate form

$$V_{[0, m_{D\bar{D}^*}]}(r) = \begin{cases} \sigma r - \frac{\zeta}{r} & r \leq r_{D\bar{D}^*} \\ m_{D\bar{D}^*} - m_c - m_{\bar{c}} & r \geq r_{D\bar{D}^*} \end{cases} \quad (3)$$

where the bracket subindex $[0, m_{D\bar{D}^*}]$ indicates that this potential is only valid up to the threshold mass $m_{D\bar{D}^*} = m_D + m_{\bar{D}^*}$, and the crossing radii $r_{D\bar{D}^*}$ is defined by the continuity of the potential at the threshold as

$$\sigma r_{D\bar{D}^*} - \frac{\zeta}{r_{D\bar{D}^*}} = m_{D\bar{D}^*} - m_c - m_{\bar{c}} \quad (4)$$

This potential, corresponding to a zero screening energy interval approach, has been drawn in Fig. 2 for the same values of the parameters previously used for $V_C(r)$. As for the threshold mass we use the value

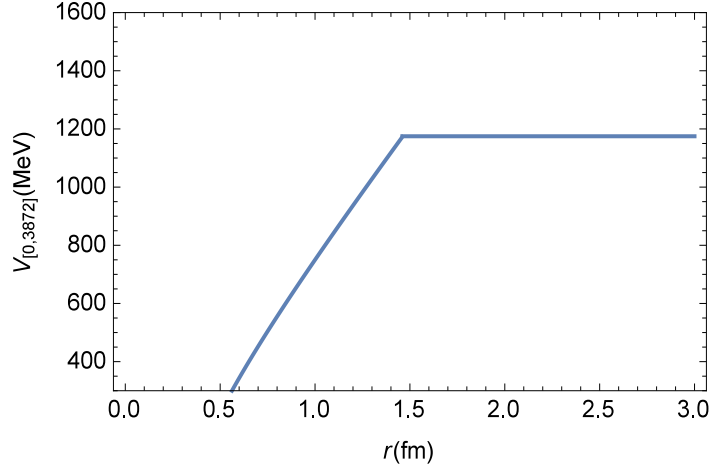


Figure 2: Representation of the $0^+(1^{++})$ $c\bar{c}$ static potential $V_{[0, m_{D\bar{D}^*}]}(r)$ with $m_c = 1348.6$ MeV, $\sigma = 850$ MeV/fm, $\zeta = 100$ MeV.fm and $m_{D\bar{D}^*} = 3872$ MeV.

$m_{D\bar{D}^*} = 3872$ MeV obtained from the experimental masses of D and \bar{D}^* [4].

The physical mechanism underlying this potential has to do with the creation of $q\bar{q}$ pairs, where q stands for a light quark ($q = u, d, s$), and the later combination of q (\bar{q}) with \bar{c} (c) giving rise to a total screening of the c and \bar{c} color charges at the threshold mass (string breaking) since the formed mesons D and \bar{D}^* are color singlets.

It is worth to remark that whereas $V_C(r)$ is defined in the whole spectral energy region the potential $V_{[0, m_{D\bar{D}^*}]}(r)$ can only be applied to calculate $0^+(1^{++})$ charmonium states with mass below the $D\bar{D}^*$ threshold mass. Therefore it is a confining potential. For higher energies the form of the $c\bar{c}$ static potential is different (one possible choice has been used to build the Generalized Screened Potential Model [13]).

To get the low lying $0^+(1^{++})$ charmonium spectrum up to $m_{D\bar{D}^*}$ we solve the Schrödinger equation for $V_{[0, m_{D\bar{D}^*}]}(r)$. The results obtained are listed in Table 1. Notice that we assign our calculated states to spin triplet ones; the reason is that our potential is spin independent and we know that spin-spin corrections to the mass are bigger (by a factor 3) for spin singlet than for spin triplet states.

Let us realize that there is no difference between the $1p_{[0, m_{D\bar{D}^*}]}$ and the conventional $1p$ state since quite below threshold there is no difference be-

J^{PC}	States $np_{[0, m_{D\overline{D}^*}]}$	$m_{[0, m_{D\overline{D}^*}]}$ MeV	m_{PDG} MeV	m_{Cor} MeV	$V_C(r)$ States np
1^{++}					
	$1p_{[0, m_{D\overline{D}^*}]}$	3454.8	3510.66 ± 0.07	3456.2	$1p$
	$2p_{[0, m_{D\overline{D}^*}]}$	3871.7	3871.69 ± 0.17		

Table 1: Calculated $0^+ (1^{++})$ charmonium masses $m_{[0, m_{D\overline{D}^*}]}$ from $V_{[0, m_{D\overline{D}^*}]}(r)$ with $\sigma = 850$ MeV/fm, $\zeta = 100$ MeV.fm, $m_c = 1348.6$ MeV and $m_{D\overline{D}^*} = 3872$ MeV. The spectral notation $np_{[0, m_{D\overline{D}^*}]}$, where n (p) indicates the principal (orbital angular momentum) quantum number has been used for the states. Masses for experimental resonances, m_{PDG} , have been taken from [4]. Masses m_{Cor} from $V_C(r)$, up to $m_{D\overline{D}^*}$, with the same values for σ , ζ and m_c are also shown for comparison.

tween using $V_{[0, m_{D\overline{D}^*}]}(r)$ and $V_C(r)$. On the contrary there is a big difference between the $2p_{[0, m_{D\overline{D}^*}]}$ state lying below threshold and the conventional $2p$ state with mass above it ($m_{Cor}(2p) = 3911$ MeV). A justified assignment of the $2p_{[0, m_{D\overline{D}^*}]}$ state to $\chi_{c1}(3872)$ has been done elsewhere [11]. Here we just plot in Fig. 3 the $2p_{[0, m_{D\overline{D}^*}]}$ radial wave function as compared to the $2p$ radial wave function to make clear the difference between them. We observe that as a consequence of the color screening in the $2p_{[0, m_{D\overline{D}^*}]}$ state there is a flux of probability from the origin outwards as compared to the non screened case. This will be important for the numerical evaluation of the width for the electromagnetic transition between $\psi(4260)$ and $\chi_{c1}(3872)$.

3 $c\bar{c}$ Potential for $0^- (1^{--})$ states

When considering the $0^- (1^{--})$ case the simple prescription of a zero screening energy interval adopted for the construction of the potential for $0^+ (1^{++})$ states has to be refined if we want to accommodate the existing data. As said before the same approach can not give any state to be reasonably assigned to $\psi(4260)$.

For this refinement let us remind that the first $S-$ wave meson-meson threshold for $0^- (1^{--})$ states, $D\overline{D}_1$, with a threshold mass $m_{D\overline{D}_1} \simeq 4287$ MeV, corresponds to $D^0\overline{D}_1^0(2420)$ where $\overline{D}_1^0(2420)$ has a width of about 30 MeV and to $D^0\overline{D}_1^0(2430)$ where $\overline{D}_1^0(2430)$ has a larger but quite uncertain width ($384_{-75}^{+107} \pm 74$ MeV). As said before the threshold effect on the static

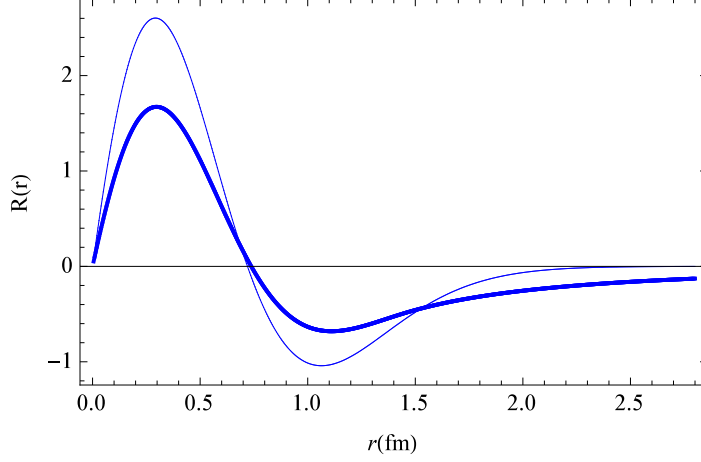


Figure 3: Radial wave functions $R(r)$ (in units $fm^{-\frac{3}{2}}$) for the $1^{++} \left(2p_{[0,m_{D\bar{D}^*}]}\right)$ state (thick line) and the $1^{++} (2p)$ state (thin line).

potential comes from the coupling of $Q\bar{Q}$ to light $q\bar{q}$ pairs out of the vacuum giving rise to the meson-meson threshold components. It turns out that in the limit $m_Q \rightarrow \infty$ the strong interaction has Heavy Quark Spin Symmetry (HQSS) and this prevents the formation of $D^0\bar{D}_1^0(2420)$ from a $Q\bar{Q}(1^{--})$ and a $q\bar{q}(0^{++})$ [16]. Therefore in this limit the only meson-meson component to be taken into account in the construction of the potential should be $D^0\bar{D}_1^0(2430)$. One should consider though that HQSS breaking is expected given the real (non infinite) mass of the charm quark, as detailed in reference [17]. Hence we shall consider $D\bar{D}_1$ as an effective threshold that may be also incorporating the possible effect of $D^0\bar{D}_1^0(2420)$. It is physically reasonable to assume that due to the non negligible widths of $\bar{D}_1^0(2430)$ and $\bar{D}_1^0(2420)$ the starting screening energy in the $0^-(1^{--})$ case is lying quite below threshold as compared to the $0^+(J^{++})$ case where the threshold widths are negligible. If we remind that for the $0^+(0^{++})$ case lattice calculations give a starting screening energy of about 30 MeV below threshold then, from the $\bar{D}_1^0(2420)$ width ($\simeq 30$ MeV), we may reasonably expect for the $0^-(1^{--})$ case the starting screening energy to be at least 60 MeV below threshold. To be more specific let us call the starting screening energy $E_s \equiv m_{D^0\bar{D}_1^0} - m_c - m_{\bar{c}} - \Delta$ where Δ indicates its distance to the threshold. Then according to our expectation $\Delta \geq 60$ MeV. On the other hand we expect Δ to be limited by a value 30 MeV bigger than the value of the $\bar{D}_1^0(2430)$ width. This determines the expected interval of possible values for

Δ . Unfortunately the uncertainty in the knowledge of the $\overline{D}_1^0(2430)$ width does not permit to fix precisely the upper bound for Δ . Instead we shall use in what follows the scarce $\psi(4260)$ data to try to fix it as much as possible. This will allow us to conclude that values of Δ within the interval $[60, 120]$ MeV may give quantitative account of the observed properties of $\psi(4260)$, see below.

The static potential will start to differ from $V_C(r)$ at E_s . To take this into account in a simple manner we shall assume that at E_s the potential reduces its slope (the one from $V_C(r)$) to a constant value s which is maintained up to the threshold mass where it becomes 0. This should be considered as an average approximation to the gradual decreasing of the slope that it is expected to really take place.

Specifically the proposed potential for $0^-(1^{--})$ states reads (again we shall assume isospin symmetry)

$$V_{[0, m_{D\overline{D}_1}]}(r) = \begin{cases} \sigma r - \frac{\zeta}{r} & r \leq r_\Delta \\ (m_{D\overline{D}_1} - m_c - m_{\overline{c}} - \Delta) + s(r - r_\Delta) & r_\Delta \leq r \leq (r_\times)_{D\overline{D}_1} \\ m_{D\overline{D}_1} - m_c - m_{\overline{c}} & r \geq (r_\times)_{D\overline{D}_1} \end{cases} \quad (5)$$

where r_Δ and $(r_\times)_{D\overline{D}_1}$ are defined by the continuity of the potential as

$$\sigma r_\Delta - \frac{\zeta}{r_\Delta} = m_{D\overline{D}_1} - m_c - m_{\overline{c}} - \Delta \quad (6)$$

$$-\Delta + s((r_\times)_{D\overline{D}_1} - r_\Delta) = 0 \quad (7)$$

Regarding the value of the slope s , we shall fix it by requiring that a bound state close below threshold appears as experimentally required by the presence of the unconventional $\psi(4260)$ resonance. It turns out that s and Δ are correlated in the sense that an increasing of Δ can be compensated by an increasing of s to get the same mass for the bound state, as can be checked in Table 2. This mitigates the lack of a clear connection between the chosen value of Δ and the real threshold widths.

It should be emphasized that for $\Delta = 0$ no bound state that could be assigned to $\psi(4260)$ can be generated. This is the quantitative translation

Δ MeV	s MeV/fm	$m_{4s[0,m_{D\overline{D}_1}]}$ MeV	$\langle r^2 \rangle^{\frac{1}{2}}$ fm
0	\times		
30	\times		
60	13	4261.5	3.7
120	64.2	4261.5	2.8
180	135	4261.5	2.5

Table 2: Correlated Δ and s values giving rise to the same mass for the $4s_{[0,m_{D\overline{D}_1}]}$ state from $V_{[0,m_{D\overline{D}_1}]}(r)$ with $\sigma = 850$ MeV/fm, $\zeta = 100$ MeV.fm, $m_c = 1348.6$ MeV and $m_{D\overline{D}_1} = 4287$ MeV. Calculated root mean square values $\langle r^2 \rangle^{\frac{1}{2}}$ are also listed. The \times sign indicates that no value of s can be found to get the required bound state.

of our previous comment about the need of going beyond the zero screening energy interval approach for $0^-(1^{--})$ states. For $\Delta \leq 30$ MeV the only possibility to generate bound states close below threshold is by choosing such a small value of s that an unphysical proliferation of bound states occur. Only for $\Delta \gtrsim 60$ MeV a well defined bound state with the required mass of 4260 MeV appears. Regarding other states than $\psi(4260)$, with masses below 4200 MeV, the different (Δ, s) pairs considered produce a rather small change in the mass of the high lying ones, of 10 MeV at most, giving rise to quite the same spectral description. (Notice that the higher the Δ value the bigger the change in the masses, what indicates that Δ cannot be much larger than 180 MeV for the same spectrum to be maintained.)

In Fig. 4 we have plotted the potential $V_{[0,m_{D\overline{D}_1}]}(r)$ for $\Delta = 60$ MeV and $s \simeq 13$ MeV/fm. As for the threshold mass we use the value $m_{D\overline{D}_1} = 4287$ MeV obtained from the experimental masses of D^0 and \overline{D}_1^0 [4]. For the remaining parameters we keep the formerly used values.

The $0^-(1^{--})$ low lying spectrum obtained from this potential is shown in Table 3.

Notice that there is almost no difference between $V_{[0,m_{D\overline{D}_1}]}(r)$ and $V_C(r)$ in the description of the (conventional) states below 4200 MeV. On the contrary

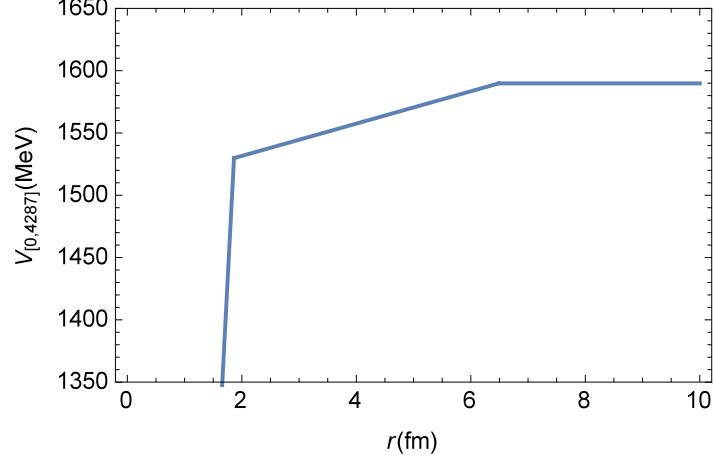


Figure 4: Representation of the $0^-(1^{--})$ $c\bar{c}$ static potential $V_{[0,m_{D\bar{D}_1}]}(r)$ with $m_c = 1348.6$ MeV, $\sigma = 850$ MeV/fm, $\zeta = 100$ MeV.fm, $m_{D\bar{D}_1} = 4287$ MeV, $\Delta = 60$ MeV and $s = 12.97$ MeV/fm.

J^{PC}	States $nl_{[0, m_{D\bar{D}_1}]}$	$m_{[0, m_{D\bar{D}_1}]}$ MeV	m_{PDG} MeV	m_{Cor} MeV	$V_C(r)$ States nl
1^{--}					
	$1s_{[0, m_{D\bar{D}_1}]}$	3046.0	3096.916 ± 0.011	3046.0	$1s$
	$2s_{[0, m_{D\bar{D}_1}]}$	3632.1	3686.09 ± 0.04	3632.2	$2s$
	$1d_{[0, m_{D\bar{D}_1}]}$	3743.4	3773.15 ± 0.33	3743.5	$1d$
	$3s_{[0, m_{D\bar{D}_1}]}$	4061.0	4039 ± 1	4065.8	$3s$
	$2d_{[0, m_{D\bar{D}_1}]}$	4136.4	4191 ± 5	4142.8	$2d$
	$4s_{[0, m_{D\bar{D}_1}]}$	4261.5	4230 ± 8		
	$3d_{[0, m_{D\bar{D}_1}]}$	4277.3			

Table 3: Calculated $0^-(1^{--})$ charmonium masses, $m_{[0, m_{D\bar{D}_1}]}$ from $V_{[0, m_{D\bar{D}_1}]}(r)$ with $\sigma = 850$ MeV/fm, $\zeta = 100$ MeV.fm, $m_c = 1348.6$ MeV and $m_{D\bar{D}_1} = 4287$ MeV. The spectral notation $nl_{[0, m_{D\bar{D}_1}]}$, where n (l) indicates the principal (orbital angular momentum) quantum number, has been used for the states. Masses for experimental resonances, m_{PDG} , have been taken from [4]. Masses m_{Cor} from $V_C(r)$, up to $m_{D\bar{D}_1}$, with the same values for σ , ζ and m_c are also shown for comparison.

from this energy to threshold the use of $V_{[0,m_{D\overline{D}_1}]}(r)$ gives rise to the appearance of the $4s_{[0,m_{D\overline{D}_1}]}$ and $3d_{[0,m_{D\overline{D}_1}]}$ states with no correspondence at all with any conventional state from $V_C(r)$ (the $4s$ state has a mass $m_{Cor}(4s) = 4437$ MeV). This allows the accommodation of $\psi(4260)$ as discussed in the next section.

For the sake of completeness it should be added that a non zero screening energy interval potential, in line with lattice results, may also be used for $0^+(1^{++})$ states. However this does not give rise to any significant difference with the zero screening energy interval approach used in Section 2. As a matter of fact for $\Delta_{1^{++}} = 30$ MeV the value of the slope can be chosen to get a completely equivalent description to the one provided by the zero screening energy interval.

4 $\psi(4260)$

In Table 3 the well established $\psi(4260)$ (different measurements of its mass go from 4222 MeV to 4284 MeV; the quoted average mass in [4] is $m_{\psi(4260)} = 4230 \pm 8$ MeV) has been assigned to the $4s_{[0,m_{D\overline{D}_1}]}$ state with a calculated mass of 4261.5 MeV although it is very probable that this state mixes with the $3d_{[0,m_{D\overline{D}_1}]}$ one giving rise a mass closer to the quoted experimental average. Under this assignment $\psi(4260)$ is an unconventional state coming out from the string breaking effect due to the $D\overline{D}_1$ threshold.

The role played by the $D\overline{D}_1(2420)$ configuration has been previously emphasized by some authors, see for example [7], [18], [19], [20], [21], [22] (and more references therein). In our potential quark model the “molecular constituents”, $D\overline{D}_1(2430)$ and $D\overline{D}_1(2420)$ are embedded in the quark-antiquark $4s_{[0,m_{D\overline{D}_1}]}$ radial wave function, drawn in Fig. 5, as reflected by the value of its root mean square radius $\langle r^2 \rangle^{\frac{1}{2}} = 3.75$ fm, much larger than for wave functions from $V_C(r)$ (for instance, $\langle r^2 \rangle^{\frac{1}{2}} = 1.55$ fm for the $4s$ state with a mass of 4437 MeV). The non vanishing probability density at long distances for the $4s_{[0,m_{D\overline{D}_1}]}$ state, say the non vanishing probability for the heavy quark and antiquark to be far apart clearly indicates that string breaking has taken place (as a related consequence the probability density at the origin has been significantly reduced).

One could argue that it is not a big deal to get the mass of a state through the fixing of the free parameter s . Nonetheless once we have the wave function of $\psi(4260)$ we can calculate its decay properties and use their

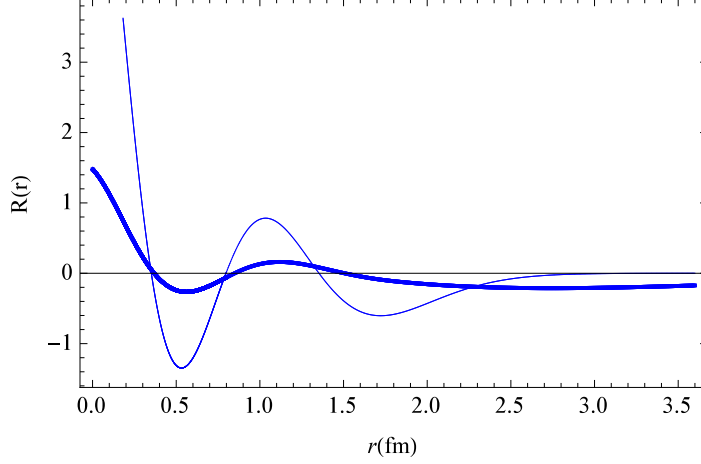


Figure 5: Radial wave functions $R(r)$ (in units $fm^{-\frac{3}{2}}$) for the $1^{--} \left(4s_{[0, m_{D\overline{D}_1}]} \right)$ state (thick line) and the $1^{--} (4s)$ state (thin line).

comparison to data as a stringent test of our effective description. In this regard let us remind that the discovery channel for $\psi(4260)$ was $J/\psi \pi^+ \pi^-$, that the conventionally dominant expected decay to $D\overline{D}$ is suppressed, that the electromagnetic decay to $\chi_{c1}(3872) \gamma$ is seen against the not seen decay to $\chi_{c1}(1p) \gamma$ and that the following ratio has been measured [4]

$$\left(\frac{\Gamma_{\psi(4260) \rightarrow J/\psi \pi^+ \pi^-} \Gamma_{\psi(4260) \rightarrow e^+ e^-}}{\Gamma_{\psi(4260)^-}} \right)_{Exp} = 9.2 \pm 1.0 \text{ eV} \quad (8)$$

It may be worth to mention that other screened potential models have been used for the description of heavy quarkonia, see for example [23], [24]. These models use a general screened potential without connection to any specific meson-meson threshold, yet generating a $4s$ state with a mass about 4260 MeV. In particular, in reference [23] an analysis of $\psi(4260)$ has been carried out (at the time of publication of reference [24] the $\psi(4260)$ had not been discovered yet). As established by the authors there are some considered difficulties, also shared by the other screened potential models of the same kind, to assign the calculated $4s$ state to $\psi(4260)$. These difficulties have to do with the experimental lack of coupling of $\psi(4260)$ to $e^+ e^-$ and with the non observation of the decay modes $D\overline{D}$, $D\overline{D}^*$ and $D^* \overline{D}^*$. Next we shall show that these difficulties are overcome in our model signaling the need to include screening effects though a detailed threshold consideration for a complete explanation of charmonium. Although we shall rely on the

particular choice $(\Delta, s) = (60 \text{ MeV}, 13 \text{ MeV/fm})$ we shall also give results for $(\Delta, s) = (120 \text{ MeV}, 64.2 \text{ MeV/fm})$ and $(\Delta, s) = (180 \text{ MeV}, 135 \text{ MeV/fm})$. This will allow us to establish the interval of variation of Δ compatible with experimental observations.

4.1 $\psi(4260) \rightarrow e^+e^-$

For conventional 3S_1 bottomonium states below their corresponding S -wave threshold the potential models we use, $V_C(r)$ and $V_{[0, m_{D\overline{D}_1}]}(r)$, reproduce quite approximately the measured ratios of leptonic widths to e^+e^- . This ratios are calculated as (see for example [25])

$$\frac{\Gamma_{i_1 \rightarrow e^+e^-}}{\Gamma_{i_2 \rightarrow e^+e^-}} = \frac{|R_{i_1}(0)|^2 m_{i_2}^2}{|R_{i_2}(0)|^2 m_{i_1}^2} \quad (9)$$

where $i_{1,2}$ stand for 3S_1 states, $R_{i_{1,2}}(0)$ for their radial wave functions at the origin and $m_{i_{1,2}}$ for their masses.

Regarding charmonium the calculated ratio $\frac{\Gamma_{2s[0, m_{D\overline{D}_1}]} \rightarrow e^+e^-}{\Gamma_{1s[0, m_{D\overline{D}_1}]} \rightarrow e^+e^-} = \frac{\Gamma_{2s \rightarrow e^+e^-}}{\Gamma_{1s \rightarrow e^+e^-}} = 0.5$ is a 15% off the experimental one $\left(\frac{\Gamma_{\psi(2s) \rightarrow e^+e^-}}{\Gamma_{J/\psi \rightarrow e^+e^-}}\right)_{Exp} = 0.42 \pm 0.02$.

Then, by assuming a similar quality for the calculated ratios involving the $4s_{[0, m_{D\overline{D}_1}]}$ state we can use

$$\frac{\Gamma_{\psi(4260) \rightarrow e^+e^-}}{\Gamma_{\psi(2s) \rightarrow e^+e^-}} \simeq \frac{\Gamma_{4s[0, m_{D\overline{D}_1}] \rightarrow e^+e^-}}{\Gamma_{2s[0, m_{D\overline{D}_1}] \rightarrow e^+e^-}} = \frac{|R_{\psi(4260)}(0)|^2 m_{\psi(2s)}^2}{|R_{\psi(2s)}(0)|^2 m_{\psi(4260)}^2} = 2.4 \times 10^{-2} \quad (10)$$

where $R_{\psi(4260)}(0) \simeq 1.5 \text{ fm}^{-\frac{3}{2}}$ and $R_{\psi(2s)}(0) \simeq 8.3 \text{ fm}^{-\frac{3}{2}}$ from our model, altogether with the experimental measurement $(\Gamma_{\psi(2s) \rightarrow e^+e^-})_{Exp} = 2.30 \pm 0.06 \text{ KeV}$ to predict an approximated leptonic decay width

$$\Gamma_{\psi(4260) \rightarrow e^+e^-} \simeq 55.2 \pm 0.2 \text{ eV} \quad (11)$$

Notice that this value is quite small as compared to $(\Gamma_{\psi(2s) \rightarrow e^+e^-})_{Exp}$ and other values for conventional states. This is a direct consequence of the lack of probability at the origin caused by screening expressed through the value of the radial wave function at the origin.

Unfortunately the $\psi(4260) \rightarrow e^+e^-$ width has not been measured separately for comparison. Instead we may use the experimentally known ratio

$$\left(\frac{\Gamma_{\psi(4260) \rightarrow J/\psi \pi^+ \pi^-} \Gamma_{\psi(4260) \rightarrow e^+ e^-}}{\Gamma_{\psi(4260)}} \right)_{Exp} = 9.2 \pm 1.0 \text{ eV} \quad (12)$$

to guess from (11) the required branching ratio

$$\frac{\Gamma_{\psi(4260) \rightarrow J/\psi \pi^+ \pi^-}}{\Gamma_{\psi(4260)}} \simeq 0.17 \pm 0.03 \quad (13)$$

Then from the total measured width

$$(\Gamma_{\psi(4260)})_{Exp} = 55 \pm 19 \text{ MeV} \quad (14)$$

we get

$$\Gamma_{\psi(4260) \rightarrow J/\psi \pi^+ \pi^-} \simeq 9 \pm 5 \text{ MeV} \quad (15)$$

It is worthwhile to point out that the leptonic width would be smaller than the estimated value (11) if $\psi(4260)$ contained also some $3d_{[0,m_{D\overline{D}_1}]}$ probability. This would make the branching ratio (13) and the decay width to $J/\psi \pi^+ \pi^-$ (15) to increase their estimated values.

For the sake of consistency $\Gamma_{\psi(4260) \rightarrow J/\psi \pi^+ \pi^-}$ should be reproduced from our quark model description. However, this calculation involves the emission of two gluons through intermediate hybrid states (see for instance [26]) that should be consistently obtained within our quark model framework. This is a task out of the scope of the present article.

Notwithstanding this we should emphasize that a small value for $\Gamma_{\psi(4260) \rightarrow e^+ e^-}$ as the one we predict is a sine qua non condition for $\psi(4260) \rightarrow J/\psi \pi^+ \pi^-$ having a significant branching ratio as required from being the discovery channel. (Just for comparison, if we had used the $4s$ wave function to describe $\psi(4260)$ the derived branching ratio would have been 0.005.) Furthermore, our predicted $\Gamma_{\psi(4260) \rightarrow e^+ e^-}$ is in line with the experimental suppression of S - wave $D\overline{D}_1$ production in e^+e^- annihilation.

To study the dependence of these results on (Δ, s) we have repeated the calculation for $(\Delta, s) = (120 \text{ MeV}, 64.2 \text{ MeV/fm})$ and $(\Delta, s) = (180 \text{ MeV}, 135 \text{ MeV/fm})$. We get $(\Gamma_{\psi(4260) \rightarrow e^+ e^-})_{(120,64.2)} \simeq 230 \pm 6 \text{ eV}$, $(\Gamma_{\psi(4260) \rightarrow J/\psi \pi^+ \pi^-})_{(120,64.2)} \simeq 2.2 \pm 1.2 \text{ MeV}$ and $(\Gamma_{\psi(4260) \rightarrow e^+ e^-})_{(180,135)} \simeq 345 \pm 9 \text{ eV}$, $(\Gamma_{\psi(4260) \rightarrow J/\psi \pi^+ \pi^-})_{(180,135)} \simeq 1.5 \pm 0.8 \text{ MeV}$. These values are still compatible with data not permitting any discrimination among the different Δ values. Incidentally, the predicted range of values for $\Gamma_{\psi(4260) \rightarrow e^+ e^-}$, $[55 \text{ eV}, 345 \text{ eV}]$, is quite similar to the one expected from a molecular model analysis [17].

4.2 E1 transitions

For conventional bottomonium and charmonium states below their corresponding S -wave thresholds the potential models we use, $V_C(r)$ and $V_{[0,m_{D\overline{D}_1}]}(r)$, give correctly the order of magnitude of the measured ratios of $^3S_1 \leftrightarrow ^3P_1$ dipole electric transitions from the same initial state or to the same final state. More accurate results are obtained if the experimental masses of the states are used instead of the calculated ones.

The theoretical expressions for these ratios are:

$$\frac{\Gamma_{E1}(i \rightarrow f_1 + \gamma)}{\Gamma_{E1}(i \rightarrow f_2 + \gamma)} = \frac{w_{if_1}^3 |D_{if_1}|^2}{w_{if_2}^3 |D_{if_2}|^2} \quad (16)$$

for the case in which the same initial state decays into two final (f_1 and f_2) states with the same value of J_f and

$$\frac{\Gamma_{E1}(i_1 \rightarrow f + \gamma)}{\Gamma_{E1}(i_2 \rightarrow f + \gamma)} = \frac{w_{i_1 f}^3 |D_{fi_1}|^2}{w_{i_2 f}^3 |D_{fi_2}|^2} \quad (17)$$

for the case in which two initial states (i_1 and i_2) decay into the same final state.

w_{if} is the photon energy and D_{if} the electric dipole matrix element

$$D_{if} = \int_0^\infty dr R_i(r) r^2 \frac{3}{w_{if}} \left[\frac{w_{if} r}{2} j_0 \left(\frac{w_{if} r}{2} \right) - j_1 \left(\frac{w_{if} r}{2} \right) \right] R_f(r) \quad (18)$$

where $R_{i,f}(r)$ are the radial wave functions of the initial and final mesons and j_0, j_1 stand for spherical Bessel functions.

By reasonably assuming the correct order of magnitude of the ratios when transitions from $4s_{[0,m_{D\overline{D}_1}]}$ are involved we predict (for $\psi(2s)$ and $\chi_{c1}(1p)$ the experimental masses are used; as for $\psi(4260)$ the calculated mass is taken since we do not consider mixing with the $3d_{[0,m_{D\overline{D}_1}]}$ state)

$$\frac{\Gamma_{\psi(4260) \rightarrow \chi_{c1}(3872)\gamma}}{\Gamma_{\psi(4260) \rightarrow \chi_{c1}(1p)\gamma}} \simeq \frac{\Gamma_{4s_{[0,m_{D\overline{D}_1}]} \rightarrow 2p_{[0,m_{D\overline{D}^*}]}\gamma}}{\Gamma_{4s_{[0,m_{D\overline{D}_1}]} \rightarrow 1p_{[0,m_{D\overline{D}^*}]}\gamma}} = 107.8 \quad (19)$$

and

$$\frac{\Gamma_{\psi(4260) \rightarrow \chi_{c1}(1p)\gamma}}{\Gamma_{\psi(2s) \rightarrow \chi_{c1}(1p)\gamma}} \simeq \frac{\Gamma_{4s_{[0,m_{D\overline{D}_1}]} \rightarrow 1p_{[0,m_{D\overline{D}^*}]}\gamma}}{\Gamma_{2s_{[0,m_{D\overline{D}_1}]} \rightarrow 1p_{[0,m_{D\overline{D}^*}]}\gamma}} = 0.018 \quad (20)$$

The first ratio (19) provides an explanation for the decay $\psi(4260) \rightarrow \chi_{c1}(3872)\gamma$ being seen against the not seen decay $\psi(4260) \rightarrow \chi_{c1}(1p)\gamma$. More quantitatively, we may use the second ratio (20) to predict from the experimental value $(\Gamma_{\psi(2s) \rightarrow \chi_{c1}(1p)\gamma})_{Exp} = 29 \pm 1 \text{ KeV}$ a width

$$\Gamma_{\psi(4260) \rightarrow \chi_{c1}(1p)\gamma} \simeq 0.506 \pm 0.017 \text{ KeV}$$

Then from the first ratio we predict

$$\Gamma_{\psi(4260) \rightarrow \chi_{c1}(3872)\gamma} \simeq 54.6 \pm 1.9 \text{ KeV}$$

We should keep in mind though that according to our assumption above these values of the widths should be considered as indicative of their order of magnitude and not as accurate predictions.

As these radiative transitions are sensitive to the details of the wave functions they can provide us, through its study from different (Δ, s) pairs, with some additional constraint on the Δ values. Actually the results we get $(\Gamma_{\psi(4260) \rightarrow \chi_{c1}(1p)\gamma})_{(120,64.2)} \simeq 1.7 \pm 0.1 \text{ keV}$, $(\Gamma_{\psi(4260) \rightarrow \chi_{c1}(3872)\gamma})_{(120,64.2)} \simeq 2.2 \pm 0.1 \text{ keV}$ and $(\Gamma_{\psi(4260) \rightarrow \chi_{c1}(1p)\gamma})_{(180,135)} \simeq 2.9 \pm 0.1 \text{ keV}$, $(\Gamma_{\psi(4260) \rightarrow \chi_{c1}(3872)\gamma})_{(180,135)} \simeq 0.044 \pm 0.004 \text{ keV}$, indicate that Δ should be smaller than 120 MeV in order not to contradict the fact that the decay $\psi(4260) \rightarrow \chi_{c1}(3872)\gamma$ is seen whereas the $\psi(4260) \rightarrow \chi_{c1}(1p)\gamma$ decay is not. Hence we may tentatively delimit the Δ interval to $[60 \text{ MeV}, 120 \text{ MeV}]$.

4.3 $\psi(4260) \rightarrow D\bar{D}$

Other issue about $\psi(4260)$ has to do with the experimental suppression of the $D\bar{D}$ decay mode despite the fact that $\psi(4260)$ is above the $D\bar{D}$ threshold mass. In order to calculate this decay we shall rely on the 3P_0 decay model [27, 28] where the physical mechanism involved is related to the one we have used to take into account color screening in the potential (a $q\bar{q}$ created in the hadronic vacuum with 0^{++} quantum numbers combines with $\bar{c}c$ giving rise to $D\bar{D}$). This model provides sensible results for the $D\bar{D}$ decay of the low lying conventional bottomonium and charmonium states with mass above the $D\bar{D}$ threshold [29].

Specifically the expression for the width is

$$\Gamma_{\psi(4260) \rightarrow D\bar{D}} = 2\pi \frac{E_D E_{\bar{D}}}{m_{\psi(4260)}} k |A|^2 \quad (21)$$

where E_D ($= E_{\bar{D}}$) is the energy of the D (or \bar{D}) meson given by

$$E_D = \sqrt{m_D^2 + k^2} = E_{\bar{D}} \quad (22)$$

being k the modulus of the three-momentum of D (or \overline{D}) for which we shall use the relativistic expression

$$k = \frac{\sqrt{(m_{\psi(4260)}^2 - 4m_D^2)}}{2} \quad (23)$$

and A stands for the decay amplitude given by

$$|A|^2 \equiv \beta^2 |\mathcal{M}|^2 \quad (24)$$

where the constant β specifies the strength of the pair creation, and the expression for $|\mathcal{M}|^2$ can be derived from [29] in a straightforward manner (we use the same notation as in this reference) as

$$|\mathcal{M}|^2 = \frac{1}{96} I(+)^2 \quad (25)$$

where

$$I(+)^2 = \left| \left[p j_1\left(\frac{pr_X}{\hbar}\right) j_1\left(\frac{\frac{1}{\hbar^2} \int_0^\infty r_X^2 dr_X \psi_X(r_X) \int p^2 dp \tilde{u}_D(p) \tilde{u}_{\overline{D}}(p)}{(m_c+m_q)\frac{kr_X}{\hbar}}\right) + \frac{m_q}{(m_c+m_q)} k j_0\left(\frac{pr_X}{\hbar}\right) j_0\left(\frac{\frac{m_c}{(m_c+m_q)} kr_X}{\hbar}\right) \right] \right|^2 \quad (26)$$

$m_q = 340$ MeV is the mass of the light quark, ψ_X denotes the radial wave function of $\psi(4260)$ in configuration space and $\tilde{u}_D(p)$ stands for radial wave function of D in momentum space

$$\tilde{u}_D(p) \equiv \sqrt{\frac{2}{\pi}} \int_0^\infty r_D^2 dr_D \psi_D(r_D) j_0\left(\frac{pr_D}{\hbar}\right) \quad (27)$$

calculated from ψ_D , the radial wave function of D in configuration space.

In order to simplify the calculation we shall approach as usual $\psi_D(r_D)$ by a gaussian (the same expression for $\psi_{\overline{D}}(r_{\overline{D}})$)

$$\psi_D(r_D) = \frac{2}{\pi^{\frac{1}{4}} R_D^{\frac{3}{2}}} e^{-\frac{r_D^2}{2R_D^2}} \quad (28)$$

R_D can be fixed either variationally or by requiring it to be equal to the root mean square (rms) radius obtained from the description of (conventional) D with $V_C(r)$ and a light quark mass of about 340 MeV (this implies a change of the value of the coulomb strength ζ to get the spectral mass). By using the rms radius procedure we get $R_D = 0.54$ fm. Then the use of the gaussian instead of the wave function from $V_C(r)$ hardly makes any difference.

We may avoid the dependence on the constant β by taking the ratio with some other $D\bar{D}$ decay process. Furthermore if the width for this other process has been measured then we can give a prediction for $\Gamma_{\psi(4260) \rightarrow D\bar{D}}$ by assuming that the calculated ratio approximates the experimental one. These conditions may be satisfied by choosing the process $\psi(3770) \rightarrow D\bar{D}$. (Notice that $\psi(3770)$ has been assigned to the $1d_{[0,m_{D\bar{D}_1}]}$ state in Table 3.)

The $\psi(3770) \rightarrow D\bar{D}$ width is given by

$$\Gamma_{\psi(3770) \rightarrow D\bar{D}} = 2\pi \frac{E'_D E'_{\bar{D}}}{m_{\psi(3770)}} k' |A'|^2$$

with

$$k' = \frac{\sqrt{(m_{\psi(3770)}^2 - 4m_D^2)}}{2}$$

and $|A'|^2 \equiv \beta^2 |\mathcal{M}'|^2$ with

$$|\mathcal{M}'|^2 = \frac{1}{48} I(-)^2$$

and

$$I(-)^2 = \left| \left[-p j_1\left(\frac{pr_X}{\hbar}\right) j_1\left(\frac{\frac{m_c}{(m_c+m_q)} k' r_X}{\hbar}\right) + \frac{m_q}{(m_c+m_q)} k' j_0\left(\frac{pr_X}{\hbar}\right) j_2\left(\frac{\frac{m_c}{(m_c+m_q)} k' r_X}{\hbar}\right) \right] \right|^2$$

where ψ'_X denotes the radial wave function of $\psi(3770)$ in configuration space.

By making use of these expressions we get (the experimental mass for $\psi(3770)$ has been used)

$$\frac{\Gamma_{\psi(4260) \rightarrow D\bar{D}}}{\Gamma_{\psi(3770) \rightarrow D\bar{D}}} = 7 \times 10^{-3}$$

that explains the $D\bar{D}$ decay suppression for $\psi(4260)$ as compared to the conventional $\psi(3770)$ state. Quantitatively, using this ratio and the measured values

$$\left(\Gamma_{\psi(3770) \rightarrow D\bar{D}}\right)_{Exp} = 25.6 \pm 0.8 \text{ MeV}$$

and

$$\left(\Gamma_{\psi(4260)}\right)_{Exp} = 55 \pm 19 \text{ MeV}$$

we predict

$$\Gamma_{\psi(4260) \rightarrow D\bar{D}} \simeq 0.18 \pm 0.01 \text{ MeV}$$

and

$$\frac{\Gamma_{\psi(4260) \rightarrow D\bar{D}}}{(\Gamma_{\psi(4260)})_{Exp}} \simeq (3 \pm 2) \times 10^{-3}$$

Regarding the dependence on the constrained (Δ, s) interval we get $\left(\Gamma_{\psi(4260) \rightarrow D\bar{D}}\right)_{(120, 64.2)} \simeq 1.7 \pm 0.1$ MeV, which is still suppressed with respect to $\Gamma_{\psi(3770) \rightarrow D\bar{D}}$ by a factor 15. Hence we may expect the experimental suppression factor to be comprised in the interval [143, 15]. To go beyond in the determination of this factor one should make use of it to calculate how the cross section $\sigma(e^+e^- \rightarrow D\bar{D})$ differs at centre of mass energies of 3770 MeV and 4260 MeV. Then, through a comparison to the measured values of $R = \frac{\sigma_{tot}(e^+e^- \rightarrow hadrons)}{\sigma_{QED}(e^+e^- \rightarrow \mu^+\mu^-)}$ at these energies [30], a more precise value of the factor might be estimated. This is a quite interesting program but clearly out of the scope of this article.

5 Summary

Starting from lattice results for the energy of two static color sources (Q and \bar{Q}) when mixing of the $Q\bar{Q}$ configuration with an open flavor meson-meson one is taken into account the form of a Born-Oppenheimer quark-antiquark static potential can be prescribed. This potential contains implicitly the effect of color screening due to the presence of light $q\bar{q}$ pairs that combine with $Q\bar{Q}$ giving rise to meson-meson components.

A simplified prescription corresponding to consider that screening takes place just at the meson-meson threshold energy, previously used for the description of $0^+(J^{++})$ charmonium ($J = 0, 1, 2$), has been refined by the introduction of a non zero screening energy interval to deal with $0^-(1^{--})$ states below their first S - wave meson-meson threshold. The spectrum from the resulting potential contains conventional like states as well as unconventional ones. This allows for the theoretical accommodation of the experimentally well established resonance $\psi(4260)$ through its assignment to a calculated state. To check the viability of such an assignment we have calculated e^+e^- , $E1$ and $D\bar{D}$ decay widths. Our results show full compatibility with existing data although more refined measurements would be needed for a more detailed comparison. Meanwhile we may tentatively conclude that $\psi(4260)$ may be described as an unconventional state coming out from the string breaking effect due to $D\bar{D}_1$ meson-meson components.

This work has been supported by Ministerio de Economía y Competitividad of Spain (MINECO) and EU Feder grant FPA2016-77177-C2-1-P and by

SEV-2014-0398. R. B. acknowledges the Ministerio de Ciencia, Innovación y Universidades of Spain for a FPI fellowship.

References

- [1] E. Eichten, K. Gottfried, T. Kinoshita, K. D. Lane and T. M. Yan, Phys. Rev. D **17**, 3090 (1978); Phys. Rev. D **21**, 203 (1980).
- [2] E. J. Eichten, K. D. Lane and C. Quigg, Phys. Rev. D **69**, 094019 (2004).
- [3] S. Godfrey and N. Isgur, Phys. Rev. D **32**, 189 (1985).
- [4] M. Tanabashi et al. (Particle Data Group (PDG)), Phys. Rev. D **98**, 030001 (2018).
- [5] H-X. Chen, W. Chen, X. Liu and S-L. Zhu, Phys. Rep. 639, 1 (2016).
- [6] R. F. Lebed, R. E. Mitchell and E. S. Swanson, Prog. Part. Nuc. Phys. **93**, 143 (2017).
- [7] F-K. Guo, C. Hanhart, U-G. Meissner, Q. Wang, Q. Zhao, B-S. Zou, Rev. Mod. Phys. **90**, 015004 (2018).
- [8] A. Esposito, A. Pilloni, A. D. Polosa, Phys. Rep. **668**, 1 (2017).
- [9] N. Brambilla *et al.*, Eur. Phys. J. C **71**, 1534 (2011).
- [10] G. S. Bali, H. Neff, T. Düssel, T. Lippert and K. Schilling (SESAM Collaboration), Phys. Rev. D **71**, 114513 (2005).
- [11] P. González, Phys. Rev. D **92**, 014017 (2015).
- [12] P. González, J.Phys. G44, 075004 (2017).
- [13] P. González, J.Phys. G 41, 095001 (2014).
- [14] E. Braaten, C. Langmack and D. H. Smith, Phys. Rev. D **90**, 014044 (2014).
- [15] G. S. Bali, Phys. Rep. **343**, 1 (2001).
- [16] X. Li and M. B. Voloshin, Phys. Rev. D **88**, 034012 (2013).
- [17] Q. Wang, M. Cleven, F-K. Guo, C. Hanhart, U-G. Meissner, X-G. Wu and Q. Zhao, Phys. Rev. D **89**, 034001 (2014).

- [18] J. L. Rosner, Phys. Rev. D **74**, 076006 (2006).
- [19] G. J. Ding, Phys. Rev. D **79**, 014001 (2009).
- [20] Q. Wang, C. Hanhart and Q. Zhao, Phys. Rev. Lett. **111**, 132003 (2013).
- [21] F. K. Guo, C. Hanhart, U. G. Meissner, Q. Wang and Q. Zhao, Phys. Lett. B **725**, 127 (2013).
- [22] W. Qin, S-R. Xue and Q. Zhao, Phys. Rev. D **94**, 054035 (2016).
- [23] B-Q Li and K-T Chao, Phys. Rev. D **79**, 094004 (2009).
- [24] P. González, A. Valcarce, H. Garcilazo, and J. Vijande, Phys. Rev. D **68**, 034007 (2003).
- [25] E. Eichten, S. Godfrey, H. Mahlke, and J. L. Rosner, Rev. Mod. Phys. **80**, 1161 (2008).
- [26] Y-P. Kuang, Int. J. Mod. Phys. A **24** S1, 327 (2009).
- [27] A. Le Yaouanc, L. Oliver, O. Pène and J. C. Raynal in "Hadron transitions in the quark model", Gordon and Breach Science Publishers 1988; Phys. Rev. D **8**, 2223 (1973).
- [28] A. Le Yaouanc, L. Oliver, O. Pene and J-C. Raynal, Phys. Lett. B **71**, 397 (1977).
- [29] S. Ono, Phys. Rev. D **23**, 1118 (1981).
- [30] J. Z. Bai *et al.* (BES), Phys. Rev. Lett. **88**, 101802 (2002).